RSC Advances

PAPER

View Article Online
View Journal | View Issue

Cite this: *RSC Adv.*, 2018, **8**, 24116

Facile access to regio- and stereoselective synthesis of highly functionalized spiro[indoline-3,2′-pyrrolidines] incorporating a pyrene moiety: experimental, photophysical and theoretical approach†

Essam M. Hussein,[ab] Ziad Moussa,[c] Nizar El Guesmi[ad] and Saleh A. Ahmed *[ab]

The regio- and stereochemical polar [3 + 2] cycloaddition of azomethine ylides, which were generated *in situ* by the reaction of isatin and sarcosine or benzylamine, with (*E*)-3-aryl-1-(pyren-1-yl)prop-2-en-1-ones as dipolarophiles, was studied using experimental and theoretical methods. The chemical structures and relative configurations of all products have been fully established by 1D and 2D homonuclear and heteronuclear correlation NMR spectrometry. The effects of the electronic and steric factors of the reactions were discussed. The photophysical properties of the synthesized spiro[indoline-3,2′-pyrrolidin]-2-ones and 5′-phenyl-spiro[indoline-3,2′-pyrrolidin]-2-ones were studied. The mechanism of the reactions was investigated using global and local reactivity indices and frontier molecular orbital (FMO) analysis at the B3LYP/6-31G level of theory. The relationship between the electrophilicity index ω of the dipolarophiles and the Hammett constant σ_p has been studied. The theoretical scale of reactivity correctly explains the electrophilic activation/deactivation effects promoted by electron-withdrawing and electron-releasing substituents in the *para*-position of the dipolarophiles.

Received 21st May 2018
Accepted 14th June 2018

DOI: 10.1039/c8ra04312d

rsc.li/rsc-advances

Introduction

Multistep reactions are typically associated with high cost, low yields, and complex isolation procedures that often include hazardous and costly solvents after each step. However, higher efficiency, higher reaction yields, lower cost, shorter reaction duration, and improved selectivity can be achieved by designing multicomponent reactions (MCRs), which provide access to synthesis of a massive number of compounds that have interesting biological properties using readily available starting materials.[1] Multicomponent [3 + 2] cycloaddition reactions, also known as Huisgen reactions, provide a direct and straightforward entry for the construction of many five-membered heterocyclic ring systems.[2] In the past few decades, [3 + 2] cycloaddition of azomethine ylides, which represent one of the most reactive and versatile classes of 1,3-dipoles, has been used to trap a range of dipolarophiles to construct pyrrolidine, pyrrolizine and pyrrolothiazole derivatives in a regio and stereo controlled fashion.[3] The spiro pyrrolidine-oxindole system is the core structure of several natural alkaloids and pharmacological agents such as spirotryptostatine A and B,[4] elacomine,[5] horsifiline,[6] and coreleucine.[7] The derivatives of spiropyrrolidine-oxindole have shown important biological applications such as modulation of the function of muscarinic serotonin receptor,[8] inhibition of microtubule assembly,[9] inhibition of human NK-1 receptor,[10] potent non-peptide inhibition of the p53-MDM2 protein–protein interaction,[11] poliovirus, rhinovirus 3C-proteinase inhibition,[12] as well as antidiabetic,[13] antibiotic,[14] anticonvulsant actions,[15] antibacterial, antiviral, anti-inflammatory, anticancer, and antitubercular activities.[16] Moreover, the molecular mechanism and the origins of the regioselectivity in [3 + 2] cycloaddition reaction of azomethine ylides with various dipolarophiles have been theoretically studied based on DFT reactivity indices[17] and molecular electron density theory.[18] The pyrene moiety is considered one of the most useful frameworks for the construction of fluorogenic chemosensors for a diversity of important chemical species.[19] However, there is little published work regarding the synthesis of spiroheterocyclic compounds which incorporate the pyrene moiety.[20] Herein, as a part of our research program on [3 + 2] cycloaddition reactions,[20,21] we describe the results of experimental and theoretical studies on the stereo- and

[a]*Chemistry Department of Chemistry, Faculty of Applied Science, Umm Al-Qura University, 21955 Makkah, Saudi Arabia. E-mail: saahmed@uqu.edu.sa; saleh.a.ahmed@aun.edu.eg; saleh_63@hotmail.com*

[b]*Department of Chemistry, Faculty of Science, Assiut University, 71516 Assiut, Egypt*

[c]*Department of Chemistry, Faculty of Science, Taibah University, P.O. Box 30002, Almadinah, Almunawarrah, Saudi Arabia*

[d]*Département de chimie, Faculté des Sciences de Monastir, Avenue de l'Environnement, 5019 Monastir, Tunisia*

† Electronic supplementary information (ESI) available. See DOI: 10.1039/c8ra04312d

regioselectivity of the [3 + 2] cycloaddition reaction of azomethine ylides, generated *in situ* from isatin (**1**) and sarcosine (**2**) or benzylamine (**6**), to a series of (*E*)-3-aryl-1-(pyren-1-yl)prop-2-en-1-ones **3a–f** to afford a new series of 4′-aryl-3'-(pyrene-1-carbonyl)spiro[indoline-3,2′-pyrrolidin]-2-ones **4a–f**.

Results and discussion

Synthetic strategy

The choice of an appropriate reaction medium was of key importance for the successful synthesis. Initially, the three-component reaction of isatin (**1**), sarcosine (**2**), and (*E*)-3-phenyl-1-(pyren-1-yl)prop-2-en-1-one (**3a**) as a simple model substrate was investigated to assess the feasibility of the strategy and to optimize the reaction conditions (Scheme 1). Different solvents such as 1,4-dioxane, tetrahydrofuran (THF), dichloromethane (CH_2Cl_2), acetonitrile, methanol, and ethanol under reflux conditions and were shown to have a substantial influence on the reaction yield. The results are summarized in Table 1 (entries 1–6). As can be seen from Table 1, the cycloaddition adduct **4a** was obtained as a single regioisomer in excellent yield (93%) with a comparatively short reaction time (4 h) when the reaction was carried out in ethanol (Table 1, entry 6). Moderate to poor yields of 50, 43, and 27% were obtained when 1,4-dioxane, THF, and dichloromethane were used as reaction solvents, respectively, even though the reaction time was increased to 10 h in order to drive the reaction forward (Table 1, entries 1–3).

Encouraged by this success, we extended this reaction of isatins (**1**) with sarcosine (**2**) to the remaining (*E*)-3-aryl-1-(pyren-1-yl)prop-2-en-1-ones **3b–f** under the optimized conditions. Thus, the corresponding 1′-methyl-4′-aryl-3′-(pyrene-1-carbonyl)-spiro[indoline-3,2′-pyrrolidin]-2-ones **4a–f** were smoothly synthesized in excellent yields (87–94%), and the results are summarized in Table 2. It can be seen from Scheme 1 that the nature of the substituents in aryl groups on the (*E*)-3-aryl-1-(pyren-1-yl)prop-2-en-1-ones **3a–f** had no significant effect on the final yield of the products.

Regio- and stereoselectivity

As shown in Schemes 1 and 2, the formation of **4a–f** proceeds through the generation of an azomethine ylide (dipole I), *via* the decarboxylative condensation of isatin **(1)** with sarcosine (**2**), which then undergoes [3 + 2] cycloaddition reaction with the dipolarophile (**3a–f**) in a highly regio- and diastereoselective fashion, leading to the exclusive formation of one of four possible diastereomers in all cases.

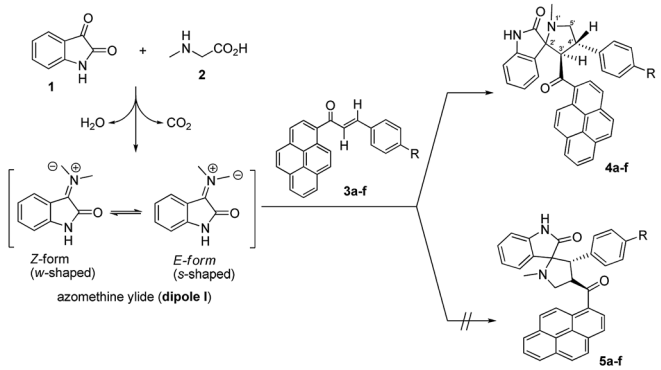

Scheme 1 Synthesis of spiro[indoline-3,2′-pyrrolidin]-2-ones **4a–f**.

Table 1 Synthetic results to **4a** under different reaction conditions[a]

Entry	Solvent	Time (h)	Yield (%)
1	Methanol	5	80
2	Ethanol	4	93
3	Acetonitrile	7	79
4	1,4-Dioxane	10	50
5	Tetrahydrofuran	10	43
6	Dichloromethane	10	27

[a] Reaction conditions: isatin (1, 1.1 mmol), sarcosine (2, 1.1 mmol), (*E*)-3-phenyl-1-(pyren-1-yl)prop-2-en-1-one (**3a**, 1.0 mmol), solvent (10 mL)/reflux.

The cycloaddition reaction is regioselective where the electron-rich carbon atom of the dipole reacts with the β-carbon of the α,β-unsaturated moiety of the dipolarophile **3a–f**. The regioselectivity in the product formation can be explained by considering the electronic effect due to resonance and the electron-withdrawing effect of the carbonyl group of the dipolarophile **3a–f** causing the β-carbon to be most electrophilic. In addition, the regioselectivity may be expounded by the secondary orbital interaction (SOI) of the orbital of the carbonyl group of dipolarophile **3a–f** with those of the azomethine ylide as suggested in Scheme 2. Accordingly, the observed regioisomer **4a–f** *via* path A is more favorable than the other regioisomer **5a–f** because of the secondary orbital interaction which is not possible in path B.

On the other hand, and although concerted cycloaddition reactions are inherently diastereoselective, one still expects two diastereomeric products due to the stereogenic center C_3, of which only a single isomer was obtained in all examples. Thus, in order to fully establish the chemical structures of the products and assign the relative stereochemistry of the stereocenters for the isolated diastereomer in each reaction, extensive 1D (^{1}H-, ^{13}C-, ^{13}C-DEPT-90/135-NMR), and 2D homonuclear and heteronuclear correlation NMR spectrometry experiments (^{1}H–^{1}H DQF-COSY, ^{1}H–^{1}H-TOCSY, HSQC-TOCSY, ^{13}C–^{1}H-HSQC, ^{13}C–^{1}H-HMBC, ^{1}H–^{1}H-ROESY) were conducted in DMSO-d_6 on a selection of compounds (see ESI†). Hence, using

Table 2 Synthesis of 1′-methyl-4′-aryl-3′-(pyrene-1-carbonyl)spiro[indoline-3,2′-pyrrolidin]-2-ones **4a–f**

Compd.	R	Time (h)	Yield[a]
4a	–H	4	93
4b	–Cl	5	85
4c	–Br	4	87
4d	$-OCH_3$	6	83
4e	$-NO_2$	3	94
4f	–CN	4	91

[a] Isolated yield.

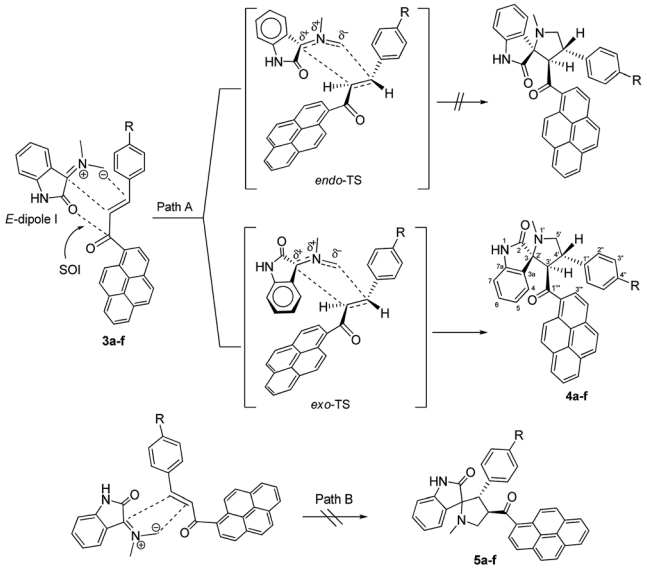

Scheme 2 Plausible mechanism for the formation of spiro[indoline-3,2′-pyrrolidin]-2-ones **4a–f**.

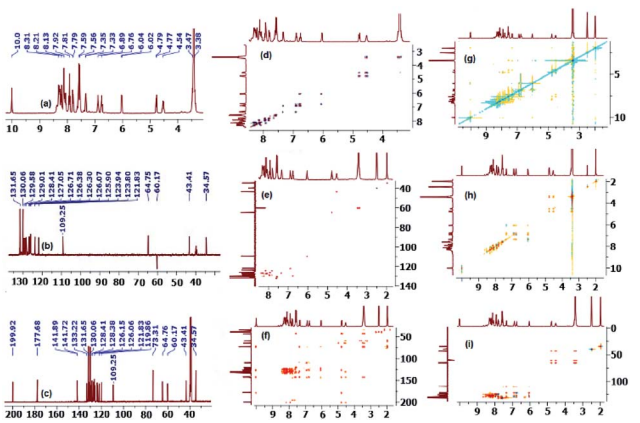

Fig. 1 (a) ^{1}H-NMR spectrum of (3*S*,3′*R*,4′*S*)-4′-(4-bromophenyl)-1′-methyl-3′-(pyrene-1-carbonyl)spiro[indoline-3,2′-pyrrolidin]-2-one (**4c**) (DMSO-d_6, 400 MHz); (b) ^{13}C-DEPT-135 spectrum (DMSO-d_6, 100 MHz), CH's (positive phase), CH_3's (positive phase), CH_2's (negative phase); (c) ^{13}C-NMR spectrum (DMSO-d_6, 100 MHz); (d) ^{1}H–^{1}H-DQFCOSY-NMR spectrum; (e) ^{1}H–^{13}C-HSQC-NMR spectrum; (f) ^{1}H–^{13}C-HMBC-NMR spectrum; (g) ^{1}H–^{1}H-ROESY-NMR spectrum; (h) TOCSY-NMR spectrum; (i) HSQC-TOCSY-NMR spectrum.

(3*S*,3′*R*,4′*S*)-4′-(4-bromophenyl)-1′-methyl-3′-(pyrene-1-carbonyl) spiro[indoline-3,2′-pyrrolidin]-2-one (**4c**) as a representative example and a model for the remaining structurally-related compounds, the relevant spectra that were used in structural elucidation and stereochemical assignment are shown in Fig. 1.

Analysis of the ^{13}C (Fig. 1, spectrum c, showing selected peak picking), ^{13}C-DEPT-90 (ESI†), and ^{13}C-DEPT-135 (Fig. 1, spectrum b) NMR spectra indicated the presence of 33 signals (15 aromatic CH's, 11 aromatic quaternary carbons, 2 carbonyl carbons, 1 quaternary sp^3 spiro-center, one methylene, one methyl, and two methine carbons) which is consistent with all carbons being nonequivalent except $C_{2''}$/$C_{3''}$. The two carbonyl carbons, one due to the ketone and another due to the indolone group appear at δ 199.9 and 177.7 ppm, respectively, and the spiro-center carbon of the pyrrolidine ring resonates most downfield (δ 73.3 ppm) among all the carbon atoms of this ring which are also the only ones with chemical shifts in the aliphatic region besides the methyl group. The peak at δ 64.8 ppm has been attribute to the C_3 carbon because the attached proton of $C_{3'}$–H (d, δ 4.78 ppm) shows strong long range ^{1}H–^{13}C heteronuclear multiple bond correlation with the adjacent ketone ($^{2}J_{CH}$) as well as with the other carbonyl group ($^{3}J_{CH}$) (Fig. 1, spectrum f) and is the most deshielded aliphatic signal due to diamagnetic anisotropy. While the methylene ^{13}C chemical shift ($C_{5'}$/δ 60.2 ppm) was clearly identified as it was the only signal with a negative phase in the ^{13}C-DEPT-135 spectrum, the attached diastereotopic protons appear as two doublets closely flanking the HOD peak (δ 3.43 ppm) and were correlated in the ^{1}H–^{13}C-HSQC-NMR spectrum by two contours to the corresponding $C_{5'}$ carbon (Fig. 1, spectrum e). Although the $C_{4'}$–H multiplicity was expected to be a three doublets (ddd) due to the surrounding non-equivalent protons, it appeared as a highly shifted downfield quartet (δ 4.53 ppm) and was correlated to the carbon at δ 43.4 ppm. The non-equivalent pyrrolidine protons were correlated to the same spin system by TOCSY (16-contour square in the aliphatic region, Fig. 1, spectrum h) and HSQC-TOCSY NMR (16-contour rectangle in the aliphatic region, Fig. 1, spectrum i) and the order of the chemical shifts was also confirmed by ^{1}H–^{1}H-DQFCOSY (Fig. 1, spectrum d). Clearly, the magnetic anisotropic effect impacted the chemical shifts for the pyrrolidine carbons and more so for its protons and outweighed the local atomic environment effect which warranted the above detailed NMR studies. Surprisingly, the –NH group of the indolone moiety (δ 10.0 ppm/^{1}H NMR, Fig. 1, spectrum a) provided the only entry point that ultimately led to the unambiguous assignment of the correct stereochemistry for the isolated diastereomer. In the ROSEY spectrum (Fig. 1, spectrum g) there exists a strong correlation cross peak between the –NH proton (δ 10.0 ppm) and H-7 (doublet, δ 6.03 ppm) and identification of the latter triggers the assignment of all the indolone ring protons. Hence, while TOCSY (16-contour square in the aromatic region, Fig. 1, spectrum h) and HSQC-TOCSY NMR (16-contour rectangle in the aromatic region, Fig. 1, spectrum i) correlated the remaining three protons in the indolone spin system (δ 7.33, δ 6.89, δ 6.76 ppm) with δ 6.03 ppm, ^{1}H–^{1}H-DQFCOSY (Fig. 1, spectrum d) was used to assign their relative position on the aromatic ring. From the ^{1}H–^{1}H-COSY correlation of H-7 (off diagonal cross peak at δ 6.03/6.76), the triplet at δ 6.76 was assigned to the adjacent proton H-6. Further, from the correlation of the latter, as evident from the contour at δ 6.76/6.89, the triplet at δ 6.89 was assigned to the neighboring H-5 proton. A last cross peak at δ 6.89/7.33 correlated the doublet at δ 7.33 which was assigned to H-4. Having assigned the chemical shifts for the indolone and pyrrolidine protons, what remained was to examine the ROSEY spectrum for any significant spatial proximity contours that could be used to assign the relative stereochemistry of the three chiral centers.

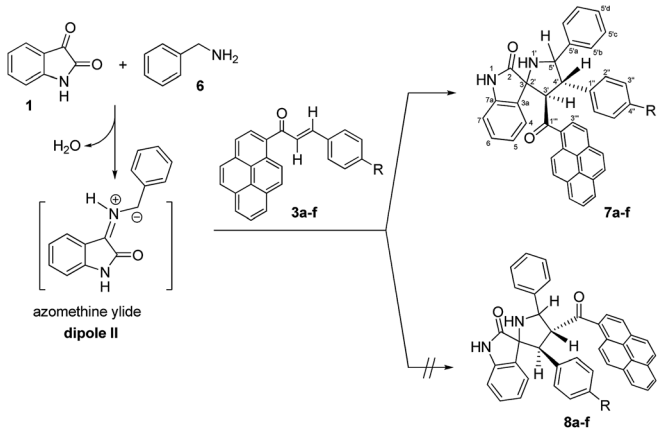

Scheme 3 Synthesis of 4′-(aryl)-5′-phenyl-3′-(pyrene-1-carbonyl)-spiro[indoline-3,2′-pyrrolidin]-2-ones **7a–f**.

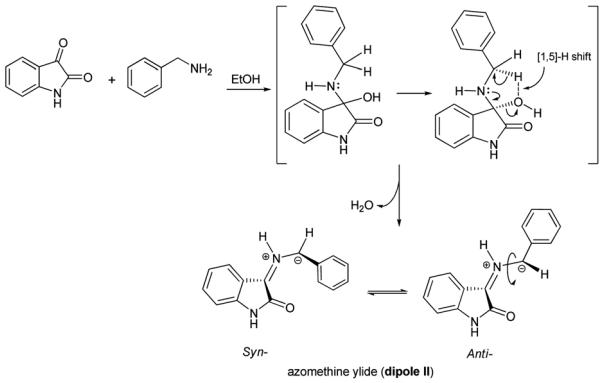

Scheme 4 Pseudo-pericyclic [1,5]-H shift approach to *syn*- and *anti*-azomethine ylide (dipole II).

Indeed, a very strong cross peak at δ 7.33/4.53 indicated the close proximity of H-4 to H-4′ which signified a *syn*-relationship between the indolinone aromatic ring and H-4′ and set the relative stereochemistry for the spirocenter (C_3/$C_{2'}$) and $C_{4'}$. The *syn*-geometry of H-3′ and the $C_{4'}$ *p*-bromophenyl moiety was evident from the off diagonal cross peak at δ 4.78/7.55 between $C_{2''}$–H (δ 7.55) and H-3′ (δ 4.78).

As suggested in Scheme 2 (path A), the formation of cycloaddition products **4a–f** proceeds *via* an "*exo*"-transition state.[22] This can be explained by the fact that the corresponding "*endo*"-transition state would require more free energy of activation than the "*exo*"-transition state due to the electrostatic repulsion between the *cis* carbonyl groups increasing the free energy of activation.[22]

To expand the scope of this three-component [3 + 2] cycloaddition reaction, the reaction of (*E*)-3-aryl-1-(pyren-1-yl)prop-2-en-1-ones **3a–f** with a non-stabilized azomethine ylide generated from isatin (**1**) and benzylamine (**6**) rather than sarcosine (**2**) was attempted. The corresponding 4′-(aryl)-5′-phenyl-3′-(pyrene-1-carbonyl)-spiro[indoline-3,2′-pyrrolidin]-2-ones **7a–f** were obtained regioselectively in good yields and the results are summarized in Scheme 3 (Table 3).

Although the detailed mechanism of the above reaction is not fully clear, the formation of regioisomer **7a–f** could be explained as follows: there are two possible isomeric structures of the azomethine ylide (dipole II), "*syn*-"' and "*anti*-" would be formed from the reaction of isatin and benzylamine *via* pseudo-pericyclic [1,5]-hydrogen shift and subsequent deprotonation[23] (Scheme 4) which then undergoes [3 + 2] cycloaddition reaction with the dipolarophile (**3a–f**) regioselectively as shown in Scheme 5 (path A). As mentioned, the observed regioisomer **7a–f** *via* path A is more favorable than the other regioisomer **8a–f** because of electronic effect and the secondary orbital interaction which is not possible in path B.

Table 3 4′-(aryl)-5′-phenyl-3′-(pyrene-1-carbonyl)spiro[indoline-3,2′-pyrrolidin]-2-ones **7a–f**

Compd.	R	Time (h)	Yield[a]
7a	–H	5	88
7b	–Cl	5	80
7c	–Br	4	85
7d	$-OCH_3$	7	70
7e	$-NO_2$	3	89
7f	–CN	4	81

[a] Isolated yield.

Similarly, the [3 + 2] cycloaddition of azomethine ylide (dipole II) to variously substituted (*E*)-3-aryl-1-(pyren-1-yl)prop-2-en-1-ones was highly diastereoselective, affording one of four possible diastereomers (8 diastereomers would be expected if the cycloaddition reaction was not inherently diastereoselective) in all cases as shown in Scheme 5. While the reaction of the electron-rich carbon atom of the dipole II with the β-carbon of the dipolarophile **3a–f** set the regiochemical outcome, determining stereoselectivity required extensive 1D and 2D NMR analysis. Using (3*S*,3′*R*,4′*S*,5′*R*)-4′-(4-nitrophenyl)-5′-phenyl-3′-(pyrene-1-carbonyl)spiro[indoline-3,2′-pyrrolidin]-2-one (**7e**) as a representative example, the relative stereochemistry of the four chiral centers was set using the same techniques as before (see ESI†). However, in order to evade undertaking detailed discussions, only the most relevant correlations will be highlighted. Strong diamagnetic anisotropic effect stemming from the newly added benzene ring at $C_{5'}$ caused unexpected strong deshielding to H-5′ (δ 5.04, J = 10.3 Hz) which was used as key to assign the remaining protons of the pyrrolidine ring. In some compounds (*e.g.* **7a**, **7f**) and under dilute conditions in DMSO-d_6, H-5′ and the pyrrolidine $N_{1'}$–H (δ 4.02–4.05) couple with each other and appear as a dd (J = 4.90–5.40 Hz for the smaller coupling constant) and *d* (J = 5.10–5.40 Hz), respectively, and were identified based on this observation. Long range ^{13}C–^{1}H-HMBC also corroborated this assignment by showing a cross peak between $N_{1'}$–H ($^2J_{CH}$) and $C_{5'}$. Accordingly, the chemical shifts for the other pyrrolidine protons were traced to δ 5.17 (3′-H) (d, J = 11.2 Hz) and 4.33 (4′-H) (t, J = 10.7 Hz) based on ^{1}H–^{1}H–COSY, ^{1}H–^{1}H-TOCSY, and HSQC-TOCSY analysis. It is noted that the chemical shifts for the indolone protons had the same order as determined before and showed the key contour between the –NH proton (δ 9.97 ppm) and H-7

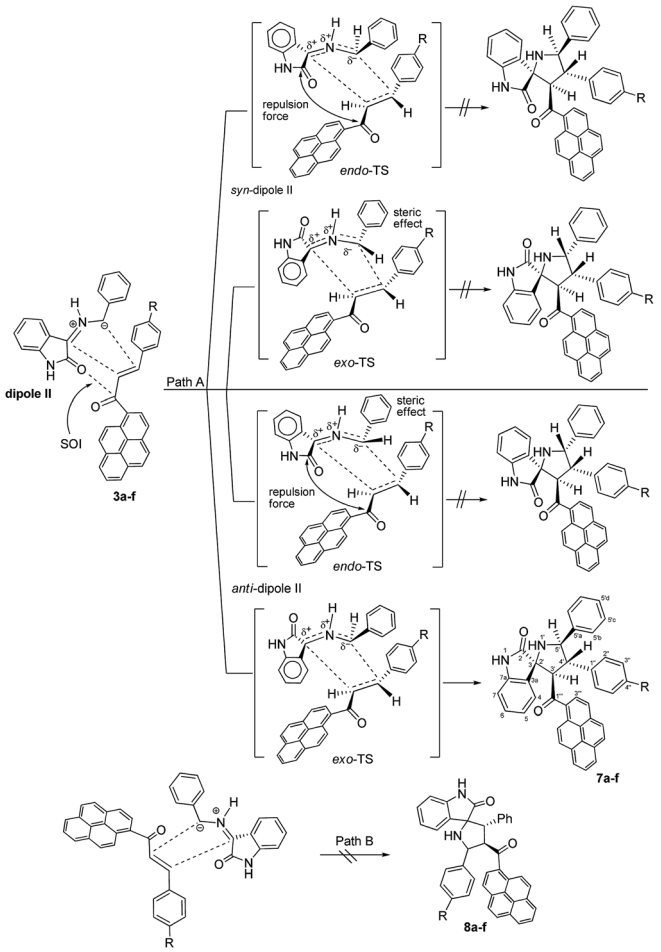

Scheme 5 Plausible mechanism for the formation of 4′-(aryl)-5′-phenyl-3′-(pyrene-1-carbonyl)spiro[indoline-3,2′-pyrrolidin]-2-ones **7a–f**.

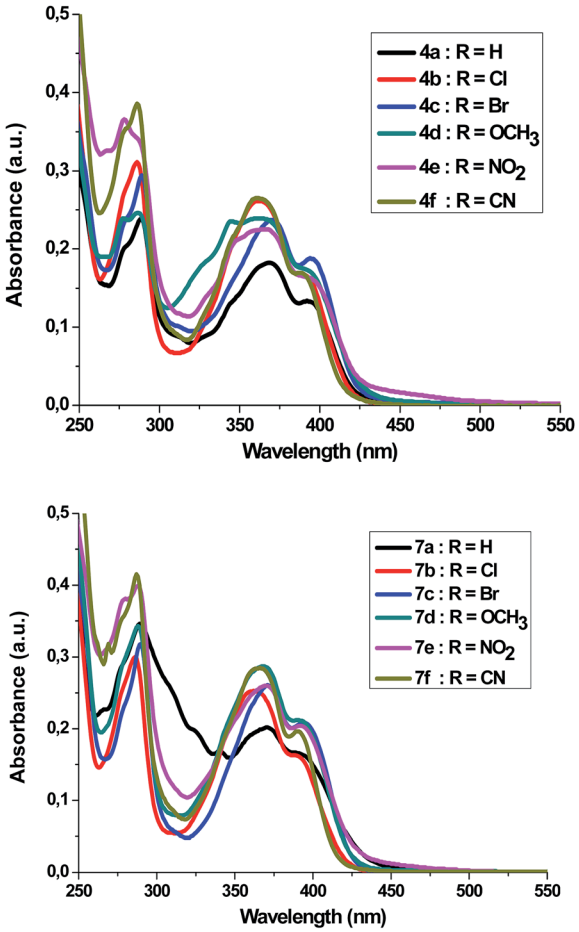

Fig. 2 UV-Vis-spectrum of **4a–f** and **7a–f** in dichloromethane ($c = 1 \times 10^{-5}$ mol dm^{-3}) at room temperature.

(doublet, δ 5.98 ppm) in the ROSEY spectrum. As such, the other indolone ring protons were matched with δ 6.73 for H-6, δ 6.96 for H-5, and δ 7.62 for H-4 based on various 2D spectral analysis. Finally, the relative stereochemistry of the four chiral centers was set based on ROSEY correlation cross peaks between H-4 and H-4′, and H-4′ and H-5′b, pointing to the *syn*-arrangement of these groups. On the other hand, the *syn*- geometry of H-3′, H-5′, and the $C_{4'}$ *p*-nitrophenyl ring was deduced from cross peaks between H-2″, H-3′ and H-5′.

As suggested in Scheme 5, the stereochemistry of cycloaddition products **7a–f** is described by considering the steric effect and the repulsion force. The formation of cycloaddition products **7a–f** proceeds *via anti*-form of the dipole II through the *exo*-transition state. This can be explained by the fact that the *endo*-transition state would require more free energy of activation due to both the steric effect and the electrostatic repulsion between the *cis* carbonyl groups.

Moreover, concerning the *syn*-form of the dipole II, the transition states would require more free energy of activation due to either the steric effect or the electrostatic repulsion between the *cis* carbonyl groups.

Absorption and emission spectra of spiro[indoline-3,2′-pyrrolidin]-2-ones 4a–f and 5′-phenyl-spiro[indoline-3,2′-pyrrolidin]-2-ones 7a–f

Absorption spectra of compounds **4a–f** and **7a–f** (1×10^{-5} M) were recorded in dichloromethane at ambient temperature. Representative absorption spectra of both compounds recorded in dichloromethane are shown in Fig. 2 and the corresponding spectral data are summarized Table 4. As seen in Fig. 2 the compounds **4a–f** and **7a–f** show a broad absorption band at 390–395 nm. Generally, changing the substituent group had no significant influence on the λ_{max}. The band absorption intensities (log ε) of the compounds **4a–f** and **7a–f** under investigations were found between 4.13 and 4.33 (Table 4). On excitation at 390 nm, only one emission peak is observed for both compounds **4a–f** and **7a–f**, a large red shifted emission band is observed within the wavelength range 477–482 nm for compound **4a–f** and 487–495 nm for **7a–f**. A bathochromic shift by ~10–13 nm was detected corresponding to the effect of adding the phenyl group on $C_{5'}$. On the other hand, as seen in Fig. 3, a remarkable increase in fluorescence intensity was observed when going from system **4a–f** to system **7a–f** by a factor of ~2.5. The fluorescence intensity was also observed to be weak

Table 4 UV-Vis absorption and fluorescence data of the synthesized compounds **4a–f** and **7a–f** in CH_2Cl_2 solution ($c = 1 \times 10^{-5}$ mol dm^{-3}) at room temperature

	4a–f			**7a–f**		
R	λ_{max}/nm, excitation	λ_{max}/nm, emission	log ε	λ_{max}/nm, excitation	λ_{max}/nm, emission	log ε
a; H	369; 392	479	4.13	371; 392	492	4.22
b; Cl	363; 391	482	4.22	362; 390	494	4.21
c; Br	370; 394	478	4.27	371; 394	492	4.32
d; OCH_3	362; 392	479	4.24	368; 390	493	4.33
e; NO_2	367; 395	477	4.21	370; 392	495	4.31
f; CN	361; 391	480	4.22	366; 390	487	4.29

for **4f** and **7f** (R=CN) and to be strong for **4c** and **7c** (R=Br). The fluorescence intensity of **4a–f** and **7a–f** strongly depended on the substituent.

Theoretical studies

Conceptual DFT provides different indices to rationalize and understand chemical structure and reactivity.[24] Structures of dipoles I, II and dipolarophiles 3 were minimized according to the preceding parameters and frontier molecular orbital (FMO) (ie; the Highest Occupied Molecular Orbital (HOMO) and the Lowest Unoccupied Molecular Orbital (LUMO)) analysis and global/local reactivity indices were used to predict regioselectivity.

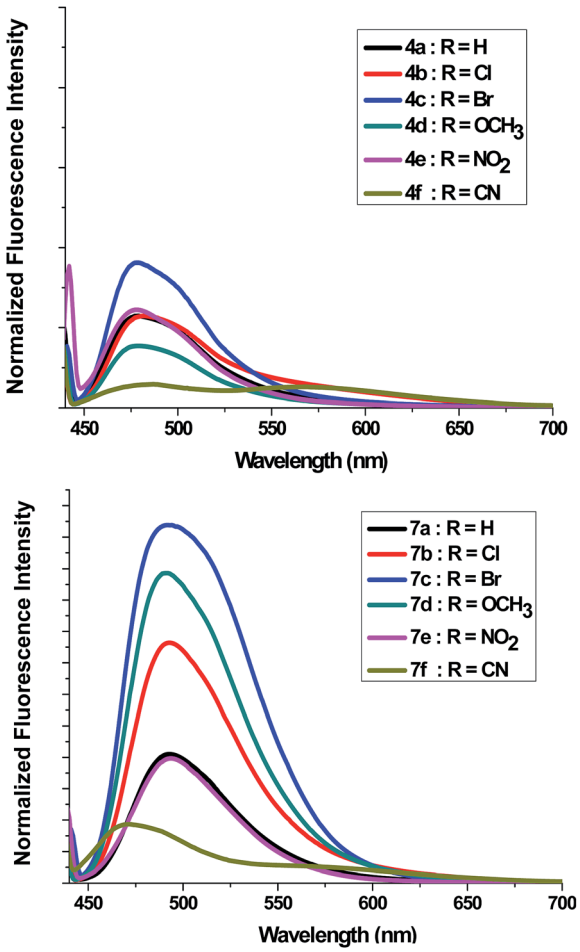

Fig. 3 Fluorescence emission spectra of **4a–f** and **7a–f** in dichloromethane ($c = 1 \times 10^{-5}$ mol dm^{-3}) at room temperature.

In this study, the HOMO–LUMO energy gaps suggest that the $LUMO_{(dipolarophile)}$–$HOMO_{(dipole)}$ interaction controls the cycloaddition reaction (normal electron demand reactions).[25] The calculated frontier orbital energies for 1,3-dipoles I, II and dipolarophiles **3a–f** are shown in Table 5. It's clear that the energy gaps $\Delta E = LUMO_{(dipolarophiles\ 3a–f)} - HOMO_{(E\text{-dipole I})}$ and $LUMO_{(dipolarophiles\ 3a–f)} - HOMO_{(anti\text{-dipole II})}$ are lower than those of the corresponding *Z*-dipole I and *syn*-dipole II, respectively.

Global reactivity indices (electronic chemical potential μ, chemical hardness η, global electrophilicity (ω)) were estimated according to the equations recommended by Parr[26] and Domingo.[27] In particular, the electronic chemical potentials and chemical hardness of the reactants studied here were evaluated in terms of the one-electron energies of the frontier molecular orbitals using the following equations: $\mu = 1/2(\varepsilon_H + \varepsilon_L)$; $\eta = (\varepsilon_L - \varepsilon_H)$.[27]

The values of μ and η were then used to calculate an important and interesting global descriptor, which is called electrophilicity index ω according to the formula

$$\omega = \mu^2/2\eta. \quad (1)$$

Electrophilicity index is a measure of the electrophilic power of a system and can be described as the maximal ability of a molecule to accept electrons in the neighborhood of an electron reservoir. Another informative index used by Domingo *et al.* is called ΔN_{max} parameter, defined by

$$\Delta N_{max} = -\mu/\eta, \quad (2)$$

which is a measure of the maximum charge transfer *i.e.* maximum amount of electronic charge that the electrophilic partner can accept.[26]

Calculated values ω, μ, η, and ΔN_{max} of relevance for the study are collected in Table 6.

The data summarized in Table 6 reveals that, the dipole I with configuration "*E*" and dipole II with configuration "*anti*" have an electronic chemical potential higher than its dipole counterparts dipole I with configuration "*Z*" and dipole II with configuration "*anti*", respectively, which means that the electronic flow is again from the azomethine ylides type dipoles to chalcones **3a–f** as dipolarophile. So, chalcones **3a–f** and acts as an electrophile due to the larger value of its ω ($1.539 < \omega < 1.858$) relatively to dipoles ω values. So, starting from the reference compound chalcone 3a (ω = 1.556 eV), the *para* substitution with chlorine (–Cl), and bromine (–Br) atoms results in an electrophilic activation in compounds chalcone **3b** (ω = 1.596 eV) and chalcone **3c** ($\omega = 1.608$ eV). The highest activation effect is achieved by electron withdrawing nitro (–NO_2) substitution, in compound chalcone **3e** (ω = 1.858 eV). In this series, the electrophilic deactivation was caused by electron releasing groups as found, for example, with the methoxy substituting –OCH_3 in compound chalcone **3d** ($\omega = 1.539$ eV). On the other

Table 5 The frontier orbital energies (eV) for dipole I, dipole II and dipolarophiles **3a–f** at the B3LYP/6-31G level of the theory

			Energy barrier (ΔE^a, eV)			
Reactant	HOMO (eV)	LUMO (eV)	*Z*-Dipole I	*E*-Dipole I	*syn*-Dipole II	*anti*-Dipole II
Z-Dipole I	−7.6259	−0.4895				
E-Dipole I	**−7.5615**	**−0.4272**				
syn-Dipole II	−7.5272	−1.1186				
anti-Dipole II	**−7.4689**	**−1.0996**				
3a	−8.2744	−1.1466	6.4793	**6.4148**	6.3806	**6.3223**
3b	−8.3236	−1.2092	6.4167	**6.3522**	6.3179	**6.2597**
3c	−8.3351	−1.2264	6.3995	**6.3350**	6.3008	**6.2425**
3d	−8.2515	−1.1197	6.5062	**6.4417**	6.4074	**6.3492**
3e	−8.4714	−1.6212	6.0047	**5.9402**	5.9059	**5.8477**
3f	−8.3876	−1.3140	6.3119	**6.2474**	6.2131	**6.1549**

[a] $\Delta E = \mathrm{LUMO}_{(\mathrm{dipolarophile})} - \mathrm{HOMO}_{(\mathrm{dipole})}$.

Table 6 Electronic chemical potential μ, chemical hardness η, global electrophilicity ω, and ΔN_{max} parameter for 1,3-dipoles I, II and dipolarophiles **3a–f**[a,b]

Reactant		μ	η	ω	ΔN_{max}
Z-Dipole I		−4.05776	7.13646	1.153	0.568
E-Ddipole I		**−3.99436**	**7.13428**	**1.118**	**0.560**
syn-Dipole II	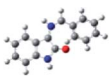	−4.32280	6.40855	1.458	0.675
anti-Dipole II		**−4.28416**	**6.36937**	**1.441**	**0.673**
3a	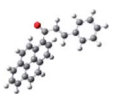	−4.71056	7.12775	1.556	0.661
3b	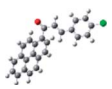	−4.76634	7.11442	1.596	0.670
3c	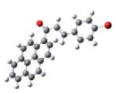	−4.78077	7.10870	1.608	0.672
3d	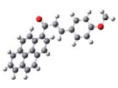	−4.68580	7.13183	1.539	0.657
3e	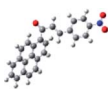	−5.04635	6.85019	1.858	0.737
3f	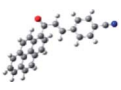	−4.85097	7.07360	1.663	0.686

[a] Electronic chemical potential μ, chemical hardness η and global electrophilicities ω in eV as defined by eqn (1); ΔN_{max} in electron units (a.u.). [b] All computations were carried out with the Gaussian 03 suite of programs. Calculations based on the method of DFT were performed using the B3LYP exchange correlation functional, together with the standard 6-31G basis set.

hand, recent investigations have used the ω values to classify dipole and dipolarophiles on a unique scale.[26–28] According to this model, the polar character of a dipole–dipolarophiles interaction can be assessed from the difference, $\Delta\omega$, in the global electrophilicities of the two reagents. It is clear that, the [3 + 2] cycloaddition of azomethine ylide I, II with chalcones **3a–f** as dipolarophiles ($\Delta\omega$ are in the range of ~0.2 and 0.7 which are ≪4.5 eV) are reactions governed by a concerted mechanism.

Relationship between the electrophilicity ω index and Hammett constant σ_p

Recently, the global electrophilicity index ω of a series of dipolarophiles is used to illustrate the rationalization of the substituent effects on the electrophilic activation/deactivation of the substrates. Indeed, aromatic substrates were chosen because of the substantial electronic effect of the *para*-substituted group on carbon–carbon double bond facilitated by the electronic transmission through the aromatic π-conjugated system.

It is known that the Hammett equation relates the relative magnitude of the equilibrium constants to a reaction constant (ρ) and a substituent constant (σ_p), according to eqn (3).[29]

$$\log(K/K_o) = \rho\sigma_p \quad (3)$$

Linear relationship between σ_p and ω have been recently obtained for *para*-substituent in the alkynes and azides series.[30] Domingo *et al.* have systematically developed a statistical procedure to obtain intrinsic electronic contributions to σ_p based on the comparison between the experimental Hammett constant σ_p and the electrophilicity index ω.

The global values of electrophilicity indexes ω for the dipolarophiles **3a–f** for the ground state of the substituting agents as well as the Hammett substituent constants σ_p are listed in Table 7.

Fig. 4 show a positive slope in the relationship between the Hammett constants σ_p of *para*-substituents in the dipolarophiles and the logarithm of the global electrophilicity ratio (ω/ω_H). It should be noted that the *para* position leads to the

Table 7 Values of the electrophilicity index σ_p for various substituents and of the logarithm of electrophilicity ratios of substituted chalcones $\log(\omega/\omega_H)$

R	σ_p	ω (eV)	$\log(\omega/\omega_H)$
–H	0.000	1.556	0.000000
–Cl	0.227	1.596	0.011023
–Br	0.232	1.608	0.014276
$-OCH_3$	−0.268	1.539	−0.004771
$-NO_2$	0.778	1.858	0.077036
–CN	0.660	1.663	0.028880

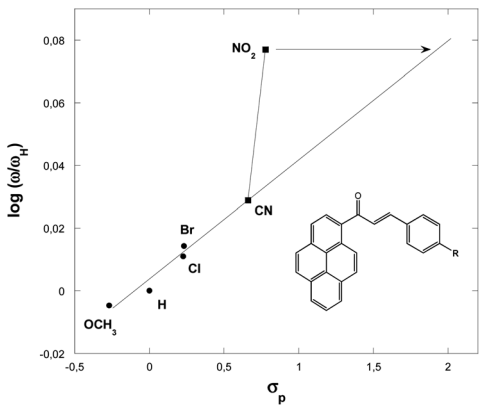

Fig. 4 Plot of the global electrophilicity ratio (ω/ω_H) against the Hammett constants for *p*-substituents in the dipolarophiles **3a–f**.

activation of the carbon–carbon double bond groups and then to a nice correlation $\log(\omega/\omega_H) = f(\sigma_p)$ for the substituent H, Cl, Br, OCH_3 and CN, while for the substituent NO_2, a remarkable deviation is observed, this deviation can be explained by the fact that the nitro group does not act with its inductive effect but by its resonance effect in which in this case $\sigma^- = 1.27$ is used and not $\sigma_p = \sim 0.78$.

The electrophilicity scale correctly accounts for the electrophilic activation/deactivation effects promoted by the substituents in the ground state of the electrophiles involved in our cycloaddition reactions. Indeed, it is proven that the electron withdrawing substituents increase the global electrophilicity of the chalcones, unlike electron releasing substituents, which behave oppositely. This behavior is due to the great activation of the chalcones carbon–carbon double bond function promoted by electronic resonance effects of the electron withdrawing substituents, instead of the great stabilization and then deactivation promoted by the electron releasing groups in the chalcones derivatives.

Conclusions

In conclusion, the regio- and stereoselective polar [3 + 2] cycloaddition reactions of azomethine ylides generated *in situ* by the reaction of isatin and sarcosine or benzylamine, with (*E*)-3-aryl-1-(pyren-1-yl)prop-2-en-1-ones as dipolarophiles were carried out to produce a new series of (3*S*,3′*R*,4′*S*)-1′-methyl-4′-aryl-3′-(pyrene-1-carbonyl)spiro[indoline-3,2′-pyrrolidin]-2-ones or (3*S*,3′*R*,4′*S*,5′*R*)-4′-(aryl)-5′-phenyl-3′-(pyrene-1-carbonyl)spiro[indoline-3,2′-pyrrolidin]-2-ones, respectively, in good to excellent yields. Absorption and emission spectral properties corresponding to **4a–f** and **7a–f** were determined in dichloromethane. Its noticeable that, substituents affect on the fluorescence behavior. Global reactivity indices for dipoles I, II and dipolarophiles **3a–f** were estimated based on the DFT/B3LYP method. It has been revealed a linear relationship between the experimental Hammett constant σ_p and the electrophilicity index ω. It can be concluded that the great activation of the dipolarophiles 3 carbon–carbon double bond function promoted by electronic resonance effects of the electron withdrawing substituents and then deactivation promoted by the electron releasing groups.

Experimental

Materials and methods

All solvents used purchased from Sigma-Aldrich are spectroscopic grade and used without further purifications. Melting points were determined on a Stuart SMP3 melting point apparatus and are uncorrected. IR spectra were recorded on a Shimadzu IR-3600 FT-IR spectrometer in KBr pellets. NMR spectra were acquired on a Bruker Avance 400 instrument (at 400 MHz for ^{1}H, 100 MHz for ^{13}C) in DMSO-d_6 solutions, using residual solvent signals as internal standards. Compounds (**3a–f**) were prepared according to described procedures.[20]

Synthetic procedures

General procedure for the synthesis of spiro[indoline-3,2′-pyrrolidin]-2-ones 4a–f. A mixture of isatin **1** (0.162 g, 1.1 mmol), sarcosine **2** (0.098 g, 1.1 mmol) and chalcone **3a–f** (1 mmol) in ethanol (10 mL) was stirred at reflux for 3–6 h and cooled to r.t. The solid formed in the reaction mixture was filtered off and recrystallized from ethanol to obtain the pure product **4a–f**.

*(3S,3′R,4′S)-1′-Methyl-4′-phenyl-3′-(pyrene-1-carbonyl)-spiro[indoline-3,2′-pyrrolidin]-2-one (**4a**).* Orange crystals; mp 124–126 °C. IR (KBr): ν_{max} = 3423 (NH), 3045 (CH arom.), 2939 (CH aliph.), 1714 (C=O), 1678 (C=O) cm^{-1}. ^{1}H NMR (400 MHz, DMSO-d_6): δ 10.10 (s, 1H, NH), 8.30 (d, J = 7.5 Hz, 1H), 8.27 (d, J = 7.5 Hz, 1H), 8.22 (d, J = 9.0 Hz, 1H), 8.15–8.03 (m, 3H), 7.94 (d, J = 9.4 Hz, 1H), 7.85 (d, J = 8.1 Hz, 1H, $C_{3'''}$–H), 7.81 (d, J = 9.2 Hz, 1H), 7.61 (d, J = 7.1 Hz, 2H, $C_{2''}$–H), 7.43 (t, J = 7.1 Hz, 2H, $C_{3''}$–H), 7.37 (d, J = 7.1 Hz, 1H, C_4–H), 7.29 (t, J = 7.4 Hz, 1H, $C_{4''}$–H), 6.93 (t, J = 7.2 Hz, 1H, C_5–H), 6.80 (t, J = 7.4 Hz, 1H, C_6–H), 6.09 (d, J = 7.4 Hz, 1H, C_7–H), 4.84 (d, J = 9.4 Hz, 1H, $C_{3'}$–H), 4.57 (q, J = 8.6 Hz, 1H, $C_{4'}$–H), 3.46–3.40 (m, 2H, $C_{5'}$–H), 2.01 (s, 3H, N–CH_3) ppm. ^{13}C NMR (100 MHz, DMSO-d_6): δ 200.2 ($C_{1'''}$), 177.9 (C_2), 142.4 ($C_{1''}$), 141.8 (C_{7a}), 133.2 (C), 131.8 (C), 130.5 (C), 129.8 (C), 129.6 (CH), 129.0 (C_6–H), 128.8 ($C_{3''}$–H), 128.4 ($C_{4''}$–H), 128.3 (C), 127.8 ($C_{2''}$–H), 127.1 (CH), 126.9 (CH), 126.7 (CH), 126.4 (C_4–H & C_{3a}), 126.3 (CH), 126.1 ($C_{3'''}$–H), 125.7 (CH), 124.0 (CH), 123.9 (CH), 123.6 (C), 123.1 (C), 121.9 (C_5–H), 109.3 (C_7–H), 73.4

($C_3/C_{2'}$), 65.0 ($C_{3'}$–H), 60.4 ($C_{5'}$–H_2), 44.2 ($C_{4'}$–H), 34.6 (N–CH_3) ppm.

*(3S,3′R,4′S)-4′-(4-Chlorophenyl)-1′-methyl-3′-(pyrene-1-carbonyl) spiro[indoline-3,2′-pyrrolidin]-2-one (**4b**).* Yellow powder; mp 157–159 °C. IR (KBr): ν_{max} = 3398 (NH), 3043 (CH arom.), 2936 (CH aliph.), 1715 (C=O), 1671 (C=O) cm^{-1}. ^1H NMR (400 MHz, DMSO-d_6): δ 10.00 (s, 1H, NH), 8.41–8.05 (m, 6H), 7.95 (d, J = 9.6 Hz, 1H), 7.92 (d, J = 8.0 Hz, 1H, $C_{3'''}$–H), 7.79 (d, J = 9.5 Hz, 1H), 7.62 (d, J = 8.3 Hz, 2H, $C_{2''}$–H), 7.47 (d, J = 8.3 Hz, 2H, $C_{3''}$–H), 7.35 (d, J = 7.3 Hz, 1H, C_4–H), 6.89 (t, J = 7.5 Hz, 1H, C_5–H), 6.78 (t, J = 7.7 Hz, 1H, C_6–H), 6.04 (d, J = 7.7 Hz, 1H, C_7–H), 4.79 (d, J = 9.5 Hz, 1H, $C_{3'}$–H), 4.55 (q, J = 8.1 Hz, 1H, $C_{4'}$–H), 3.42 (d, J = 8.6 Hz, 1H, $C_{5'}$–H), 3.38 (d, J = 8.6 Hz, 1H, $C_{5'}$–H), 1.99 (s, 3H, N–CH_3) ppm. ^{13}C NMR (100 MHz, DMSO-d_6): δ 199.9 ($C_{1'''}$), 177.7 (C_2), 141.7 ($C_{1''}$), 141.4 (C_{7a}), 133.2 (C), 131.6 ($C_{4''}$–Cl), 131.4 (C), 130.5 (C), 129.8 (C), 129.6 ($C_{2''}$–H), 129.5 (C–H), 129.0 (C_6–H), 128.7 ($C_{3''}$–H), 128.4 (C–H), 128.3 (C), 127.0 (CH), 126.7 (CH), 126.4 (C_4–H), 126.3 (CH), 126.1 (C_{3a}), 126.0 ($C_{3'''}$–H), 125.8 (CH), 123.9 (CH), 123.8 (CH), 123.6 (C), 123.1 (C), 121.8 (C_5–H), 109.3 (C_7–H), 73.3 ($C_3/C_{2'}$), 64.8 ($C_{3'}$–H), 60.2 ($C_{5'}$–H_2), 43.4 ($C_{4'}$–H), 34.6 (N–CH_3) ppm.

*(3S,3′R,4′S)-4′-(4-Bromophenyl)-1′-methyl-3′-(pyrene-1-carbonyl) spiro[indoline-3,2′-pyrrolidin]-2-one (**4c**).* Yellow powder; mp 157–159 °C. IR (KBr): ν_{max} = 3206 (NH), 3046 (CH arom.), 2935 (CH aliph.), 1716 (C=O), 1679 (C=O) cm^{-1}. ^1H NMR (400 MHz, DMSO-d_6): δ 10.02 (s, 1H, NH), 8.30 (d, J = 7.4 Hz, 1H), 8.27 (d, J = 7.7 Hz, 1H), 8.22 (d, J = 8.7 Hz, 1H), 8.17–8.03 (m, 3H), 7.93 (d, J = 9.5 Hz, 1H), 7.90 (d, J = 8.0 Hz, 1H, $C_{3'''}$–H), 7.80 (d, J = 9.7 Hz, 1H), 7.60 (d, J = 7.7 Hz, 2H, $C_{3''}$–H), 7.55 (d, J = 7.7 Hz, 2H, $C_{2''}$–H), 7.33 (d, J = 7.2 Hz, 1H, C_4–H), 6.89 (t, J = 7.4 Hz, 1H, C_5–H), 6.76 (t, J = 7.4 Hz, 1H, C_6–H), 6.03 (d, J = 7.6 Hz, 1H, C_7–H), 4.78 (d, J = 9.3 Hz, 1H, $C_{3'}$–H), 4.53 (q, J = 8.7 Hz, 1H, $C_{4'}$–H), 3.48 (d, J = 9.0 Hz, 1H, $C_{5'}$–H), 3.37 (d, J = 9.6 Hz, 1H, $C_{5'}$–H), 1.98 (s, 3H, N–CH_3) ppm. ^{13}C NMR (100 MHz, DMSO-d_6): δ 199.9 ($C_{1'''}$), 177.7 (C_2), 141.9 ($C_{1''}$), 141.7 (C_{7a}), 133.2 (C), 131.7 ($C_{3''}$–H), 131.6 (C), 130.5 (C), 130.1 ($C_{2''}$–H), 129.8 (C), 129.6 (C–H), 129.0 (C_6–H), 128.4 (C–H), 128.3 (C), 127.1 (CH), 126.7 (CH), 126.4 (C_4–H), 126.3 (CH), 126.2 (C_{3a}), 126.1 ($C_{3'''}$–H), 125.9 (CH), 123.9 (CH), 123.8 (CH), 123.6 (C), 123.1 (C), 121.8 (C_5–H), 119.9 ($C_{4''}$–Br), 109.3 (C_7–H), 73.3 ($C_3/C_{2'}$), 64.8 ($C_{3'}$–H), 60.2 ($C_{5'}$–H_2), 43.4 ($C_{4'}$–H), 34.6 (N–CH_3) ppm.

*(3S,3′R,4′S)-4′-(4-Methoxyphenyl)-1′-methyl-3′-(pyrene-1-carbonyl) spiro[indoline-3,2′-pyrrolidin]-2-one (**4d**).* Yellow powder; mp 118–120 °C. IR (KBr): ν_{max} = 3394 (NH), 3040 (CH arom.), 2934 (CH aliph.), 1717 (C=O), 1681 (C=O) cm^{-1}. ^1H NMR (400 MHz, DMSO-d_6): δ 8.61 (s, 1H, NH), 8.22–8.04 (m, 6H), 7.95 (d, J = 9.6 Hz, 2H), 7.93 (d, J = 8.0 Hz, 1H, $C_{3'''}$–H), 7.63 (d, J = 8.3 Hz, 2H, $C_{2''}$–H), 7.55 (d, J = 8.3 Hz, 2H, $C_{3''}$–H), 7.52 (d, J = 7.3 Hz, 1H, C_4–H), 6.91–6.89 (m, 2H, C_5–H, C_6–H), 6.04 (d, J = 7.7 Hz, 1H, C_7–H), 4.91 (d, J = 9.5 Hz, 1H, $C_{3'}$–H), 4.71 (q, J = 8.1 Hz, 1H, $C_{4'}$–H), 3.83 (s, 3H, O–CH_3), 3.73 (d, J = 8.6 Hz, 1H, $C_{5'}$–H), 3.56 (d, J = 8.6 Hz, 1H, $C_{5'}$–H), 2.14 (s, 3H, N–CH_3) ppm. ^{13}C NMR (100 MHz, DMSO-d_6): δ 196.3 ($C_{1'''}$), 161.8 (C_2), 158.5 ($C_{1''}$), 146.2 (C_{7a}), 133.2 ($C_{4''}$), 131.2 (C), 131.4 (C), 130.5 (C), 129.8 (C), 129.6 ($C_{2''}$–H), 129.5 (C–H), 129.0 (C_6–H), 128.7 ($C_{3''}$–H), 128.4 (C–H), 128.3 (C), 127.0 (CH), 126.7 (CH), 126.4 (C_4–H), 126.3 (CH), 126.1 (C_{3a}), 126.0 ($C_{3'''}$–H), 125.8 (CH), 124.1 (CH), 123.9 (CH), 114.4 (C), 114.2 (C), 114.0 (C_5–H), 109.6 (C_7–H), 74.2 ($C_3/C_{2'}$), 64.8 ($C_{3'}$–H), 60.9 ($C_{5'}$–H_2), 55.4 (O–CH_3), 44.0 ($C_{4'}$–H), 35.1 (N–CH_3) ppm.

*(3S,3′R,4′S)-1′-Methyl-4′-(4-nitrophenyl)-3′-(pyrene-1-carbonyl) spiro[indoline-3,2′-pyrrolidin]-2-one (**4e**).* Pale brown powder; mp 161–163 °C. IR (KBr): ν_{max} = 3340 (NH), 3047 (CH arom.), 2941 (CH aliph.), 1716 (C=O), 1680 (C=O) cm^{-1}. ^1H NMR (400 MHz, DMSO-d_6): δ 10.0 (s, 1H, NH), 8.42–7.77 (m, 11H), 7.40–7.33 (m, 3H, C_4–H and pyrene-H) 6.90 (t, J = 7.6 Hz, 1H, C_5–H), 6.75 (t, J = 7.7 Hz, 1H, C_6–H), 6.03 (d, J = 7.9 Hz, 1H, C_7–H), 4.86 (d, J = 9.0 Hz, 1H, $C_{3'}$–H), 4.71 (q, J = 8.1 Hz, 1H, $C_{4'}$–H), 3.41 (d, J = 8.6 Hz, 1H, $C_{5'}$–H), 3.37 (d, J = 8.6 Hz, 1H, $C_{5'}$–H), 1.99 (s, 3H, N–CH_3) ppm. ^{13}C NMR (100 MHz, DMSO-d_6): δ 199.6 ($C_{1'''}$), 177.4 (C_2), 146.6 ($C_{4''}$–NO_2), 146.4 ($C_{1''}$), 141.7 (C_{7a}), 133.3 (C), 131.3 (C), 130.5 (C), 129.8 (C), 129.6 (CH), 129.5 (C–H), 129.1 ($C_{2''}$–H), 129.0 (C_6–H), 128.4 (C–H), 127.0 (CH), 126.7 (C), 126.6 (CH), 126.3 (CH), 126.2 (C_4–H), 126.0 ($C_{3'''}$–H), 125.8 (C_{3a}), 123.9 ($C_{3''}$–H), 123.7 (CH), 123.5 (C), 123.1 (C), 122.8 (CH), 121.8 (C_5–H), 109.3 (C_7–H), 73.4 ($C_3/C_{2'}$), 64.6 ($C_{3'}$–H), 60.0 ($C_{5'}$–H_2), 43.6 ($C_{4'}$–H), 34.5 (N–CH_3) ppm.

*(3S,3′R,4′S)-4′-(4-Cyanophenyl)-1′-methyl-3′-(pyrene-1-carbonyl) spiro[indoline-3,2′-pyrrolidin]-2-one (**4f**).* Orange crystals; mp 150–152 °C. IR (KBr): ν_{max} = 3397 (NH), 3048 (CH arom.), 2939 (CH aliph.), 2226 (CN), 1716 (C=O), 1682 (C=O) cm^{-1}. ^1H NMR (400 MHz, DMSO-d_6): δ 10.0 (s, 1H, NH), 8.44–8.06 (m, 6H), 7.96 (d, J = 9.4 Hz, 2H), 7.89 (d, J = 7.9 Hz, 2H, $C_{3''}$–H), 7.84–7.77 (m, 3H, $C_{2''}$–H and pyrene-H), 7.36 (d, J = 7.2 Hz, 1H, C_4–H), 6.90 (t, J = 7.5 Hz, 1H, C_5–H), 6.75 (t, J = 7.6 Hz, 1H, C_6–H), 6.01 (d, J = 7.7 Hz, 1H, C_7–H), 4.82 (d, J = 9.1 Hz, 1H, $C_{3'}$–H), 4.65 (q, J = 8.0 Hz, 1H, $C_{4'}$–H), 3.56–3.36 (m, 2H, $C_{5'}$–H), 1.98 (s, 3H, N–CH_3) ppm. ^{13}C NMR (100 MHz, DMSO-d_6): δ 199.6 ($C_{1'''}$), 177.4 (C_2), 148.5 ($C_{1''}$), 141.7 (C_{7a}), 133.2 (C), 132.7 ($C_{3''}$–H), 131.3 (C), 130.4 (C), 129.7 (C), 129.5 (CH), 129.0 (C_6–H), 128.9 ($C_{2''}$–H), 128.4 (C–H & C overlapping), 127.0 (CH), 126.6 (CH), 126.3 (CH), 126.2 (C_4–H), 126.0 (CH & $C_{3'''}$–H overlapping), 125.9 (C_{3a}), 123.9 (C–H), 123.7 (CH), 123.5 (C), 123.0 (C), 121.8 (C_5–H), 118.9 (CN), 109.6 ($C_{4''}$), 109.2 (C_7–H), 73.3 ($C_3/C_{2'}$), 64.5 ($C_{3'}$–H), 60.0 ($C_{5'}$–H_2), 43.8 ($C_{4'}$–H), 34.5 (N–CH_3) ppm.

General procedure for the synthesis of 5′-diphenyl-3′-(pyrene-1-carbonyl)spiro[indoline-3,2′-pyrrolidin]-2-one 7a–f. A mixture of isatin **1** (0.162 g, 1.1 mmol), benzylamine **6** (0.117 g, 1.1 mmol) and chalcone **3a–f** (1 mmol) in ethanol (10 mL) was stirred at reflux for 3–7 h. The solid formed in the reaction mixture on hot was filtered off and recrystallized from dioxane to obtain the pure product **7a–f**.

*(3S,3′R,4′S,5′R)-4′,5′-Diphenyl-3′-(pyrene-1-carbonyl)-spiro[indoline-3,2′-pyrrolidin]-2-one (**7a**).* Orange crystals; mp 100–101 °C. IR (KBr): ν_{max} = 3347 (NH), 3291 (NH), 3029 (CH arom.), 2971 (CH aliph.), 1706 (C=O), 1675 (C=O) cm^{-1}. ^1H NMR (400 MHz, DMSO-d_6): δ 9.97 (s, 1H, N_1–H), 8.35–8.04 (m, 6H, pyrene H), 7.97–7.84 (m, 3H, pyrene H), 7.63 (d, J = 7.3 Hz, 1H, C_4–H), 7.52 (d, J = 7.6 Hz, 2H, C_{ph}–H), 7.44 (d, J = 7.5 Hz, 2H, C_{ph}–H), 7.35–7.10 (m, 6H, C_{ph}–H), 7.02 (t, J = 7.6 Hz, 1H, C_5–H), 6.83 (t, J = 7.6 Hz, 1H, C_6–H), 6.10 (d, J = 7.5 Hz, 1H, C_7–H), 5.10 (d, J = 11.1 Hz, 1H, $C_{3'}$–H), 5.05 (dd, J = 10.2, 4.9 Hz, 1H, $C_{5'}$–H), 4.22 (t, J = 10.7 Hz, 1H, $C_{4'}$–H), 4.02 (d, J = 5.1 Hz, 1H, $N_{1'}$–H) ppm. ^{13}C NMR (100 MHz, DMSO-d_6): δ 200.2 ($C_{1'''}$), 181.1 (C_2), 142.4 ($C_{1''}$),

141.4 (C_{7a}), 139.2 ($C_{5'a}$), 133.1 (C), 132.1 (C), 130.8 (C), 130.4 (C), 129.7 (C), 129.5 (C–H), 128.5 (C_6–H), 128.4 (C–H), 128.1 (C–H), 128.0 (C–H), 127.9 (C–H), 127.4 (C–H), 127.3 (C–H), 127.2 (C–H), 127.0 (C–H), 126.9 (C–H), 126.6 (C–H), 126.3 (C_4–H), 126.0 (C–H), 125.6 (C–H), 124.0 (C–H), 123.8 (C–H), 123.7 (C), 123.5 (C), 123.1 (C), 121.8 (C_5–H), 109.0 (C_7–H), 67.9 (C_3/$C_{2'}$), 67.5 ($C_{5'}$–H), 65.0 ($C_{3'}$–H), 55.9 ($C_{4'}$–H) ppm.

*(3S,3′R,4′S,5′R)-4′-(4-Chlorophenyl)-5′-phenyl-3′-(pyrene-1-carbonyl) spiro[indoline-3,2′-pyrrolidin]-2-one (**7b**).* Yellow powder; mp 180–182 °C. IR (KBr): ν_{max} = 3325 (NH), 3180 (NH), 3038 (CH arom.), 2940 (CH aliph.), 1705 (C=O), 1670 (C=O) cm^{-1}. ^{1}H NMR (400 MHz, DMSO-d_6): δ 9.96 (s, 1H, N_1–H), 8.62 (d, J = 8.0 Hz, 1H, $C_{3'''}$–H), 8.40 (d, J = 7.6 Hz, 1H), 8.32–8.25 (m, 5H), 8.10 (d, J = 8.0 Hz, 2H, $C_{3''}$–H), 8.09–8.01 (m, 2H), 7.98 (d, J = 8.6 Hz, 2H, $C_{2''}$–H), 7.94 (d, J = 7.3 Hz, 1H, C_4–H), 7.91 (d, J = 7.3 Hz, 2H, $C_{5'b}$–H), 7.84 (d, J = 7.3 Hz, 2H, $C_{5'c}$–H), 7.60–7.54 (m, 1H, $C_{5'd}$–H), 7.15 (t, J = 7.0 Hz, 1H, C_5–H), 6.75 (t, J = 7.0 Hz, 1H, C_6–H), 6.02 (d, J = 7.7 Hz, 1H, C_7–H), 5.55 (d, J = 11.0 Hz, 1H, $C_{3'}$–H), 5.01 (d, J = 11.2 Hz, 1H, $C_{5'}$–H), 4.17 (t, J = 10.8 Hz, 1H, $C_{4'}$–H), 4.01 (br, 1H, $N_{1'}$–H) ppm. ^{13}C NMR (100 MHz, DMSO-d_6): δ 200.1 ($C_{1'''}$), 180.9 (C_2), 142.9 ($C_{4''}$), 141.3 ($C_{1''}$), 139.1 (C_{7a}), 135.9 ($C_{5'a}$), 133.6 (C), 132.1 (C), 131.7 (C_{3a}), 131.2 (C), 130.6 ($C_{2''}$–H), 130.6 (C), 130.3 (C–H), 130.2 (C–H), 129.6 (C), 128.7 (C_6–H), 128.6 ($C_{5'c}$–H), 127.8 (CH), 127.6 ($C_{5'd}$–H), 127.5 ($C_{5'b}$–H), 127.1 (CH), 126.8 (C–H), 126.5 ($C_{3'''}$–H), 125.1 (C_4–H), 124.4 (CH), 124.0 (CH), 123.5 ($C_{3''}$–H), 122.4 (C), 122.3 (CH), 120.9 (C), 120.4 (C_5–H), 109.3 (C_7–H), 72.4 (C_3/$C_{2'}$), 67.5 ($C_{5'}$–H), 65.2 ($C_{3'}$–H), 55.4 ($C_{4'}$–H) ppm.

*(3S,3′R,4′S,5′R)-4′-(4-Bromophenyl)-5′-phenyl-3′-(pyrene-1-carbonyl) spiro[indoline-3,2′-pyrrolidin]-2-one (**7c**).* Yellow powder; mp 234–235 °C. IR (KBr): ν_{max} = 3345 (NH), 3327 (NH), 3036 (CH arom.), 2945 (CH aliph.), 1704 (C=O), 1670 (C=O) cm^{-1}. ^{1}H NMR (400 MHz, DMSO-d_6): δ 9.93 (s, 1H, N_1–H), 8.65 (d, J = 8.0 Hz, 1H, $C_{3'''}$–H), 8.42 (d, J = 7.6 Hz, 1H), 8.36–8.26 (m, 5H), 8.19 (d, J = 8.5 Hz, 2H, $C_{3''}$–H), 8.14–8.09 (m, 2H), 8.00 (d, J = 8.6 Hz, 2H, $C_{2''}$–H), 7.96 (d, J = 7.3 Hz, 1H, C_4–H), 7.92 (d, J = 7.3 Hz, 2H, $C_{5'b}$–H), 7.83 (d, J = 7.3 Hz, 2H, $C_{5'c}$–H), 7.60–7.53 (m, 1H, $C_{5'd}$–H), 7.16 (t, J = 7.0 Hz, 1H, C_5–H), 6.73 (t, J = 7.0 Hz, 1H, C_6–H), 6.01 (d, J = 7.7 Hz, 1H, C_7–H), 5.54 (d, J = 11.0 Hz, 1H, $C_{3'}$–H), 5.05 (d, J = 11.2 Hz, 1H, $C_{5'}$–H), 4.15 (t, J = 10.8 Hz, 1H, $C_{4'}$–H), 4.03 (br, 1H, $N_{1'}$–H) ppm. ^{13}C NMR (100 MHz, DMSO-d_6): δ 200.3 ($C_{1'''}$), 181.4 (C_2), 142.7 ($C_{4''}$), 141.8 ($C_{1''}$), 139.0 (C_{7a}), 135.9 ($C_{5'a}$), 133.7 (C), 132.1 (C), 131.9 (C_{3a}), 131.2 (C), 130.9 ($C_{2''}$–H), 130.7 (C), 130.5 (C–H), 130.2 (C–H), 129.4 (C), 128.7 (C_6–H), 128.6 ($C_{5'c}$–H), 127.8 (CH), 127.6 ($C_{5'd}$H), 127.5 ($C_{5'b}$–H), 127.1 (CH), 126.8 (C–H), 126.5 ($C_{3'''}$–H), 124.9 (C_4–H), 124.4 (CH), 124.0 (CH), 123.5 ($C_{3''}$–H), 122.4 (C), 122.3 (CH), 120.9 (C), 120.4 (C_5–H), 109.4 (C_7–H), 72.3 (C_3/$C_{2'}$), 68.2 ($C_{5'}$–H), 64.9 ($C_{3'}$–H), 55.2 ($C_{4'}$–H) ppm.

*(3S,3′R,4′S,5′R)-4′-(4-Methoxyphenyl)-5′-phenyl-3′-(pyrene-1-carbonyl)spiro[indoline-3,2′-pyrrolidin]-2-one (**7d**).* Yellow powder; mp 177–179 °C. IR (KBr): ν_{max} = 3324 (NH), 3182 (NH), 3034 (CH arom.), 2941 (CH aliph.), 1700 (C=O), 1668 (C=O) cm^{-1}. ^{1}H NMR (400 MHz, DMSO-d_6): δ 10.04 (s, 1H, N_1–H), 8.59–8.42 (m, 3H), 8.37 (d, J = 8.5 Hz, 2H, $C_{3''}$–H), 8.33–8.28 (m, 4H), 8.23–8.10 (m, 2H), 8.08 (d, J = 8.4 Hz, 2H, $C_{2''}$–H), 7.91 (d, J = 7.3 Hz, 1H, C_4–H), 7.80 (d, J = 7.3 Hz, 2H, $C_{5'b}$–H), 7.26 (d, J = 7.3 Hz, 2H, $C_{5'c}$–H), 7.12–7.10 (m, 1H, $C_{5'd}$–H), 6.69 (t, J = 7.5 Hz, 1H, C_5–H), 6.63 (t, J = 7.6 Hz, 1H, C_6–H), 5.97 (d, J = 11.6 Hz, 1H, C_7–H), 5.55 (d, J = 11.2 Hz, 1H, $C_{3'}$–H), 5.05 (d, J = 10.3 Hz, 1H, $C_{5'}$–H), 4.51 (t, J = 10.7 Hz, 1H, $C_{4'}$–H), 4.18 (br, 1H, $N_{1'}$–H), 3.60 (s, 3H, O–CH_3) ppm. ^{13}C NMR (100 MHz, DMSO-d_6): δ 201.7 ($C_{1'''}$), 181.2 (C_2), 143.2 ($C_{4''}$), 142.8 ($C_{1''}$), 133.7 (C_{7a}), 133.4 ($C_{5'a}$), 133.1 (C), 131.0 (C), 130.2 (C_{3a}), 130.0 (C), 129.4 ($C_{2''}$–H), 129.2 (C), 129.0 (C–H), 128.8 (C–H), 128.1 (C), 127.8 (C_6–H), 127.5 ($C_{5'c}$–H), 127.1 (CH), 126.8 ($C_{5'd}$H), 126.4 ($C_{5'b}$–H), 124.9 (CH), 124.4 (C–H), 124.3 ($C_{3'''}$–H), 124.2 (C_4–H), 123.9 (CH), 123.5 (CH), 122.2 ($C_{3''}$–H), 114.9 (C), 114.4 (CH), 114.0 (C), 113.8 (C_5–H), 109.6 (C_7–H), 72.4 (C_3/$C_{2'}$), 65.5 ($C_{5'}$–H), 61.3 ($C_{3'}$–H), 55.3 (O–CH_3), 54.8 ($C_{4'}$–H) ppm.

*(3S,3′R,4′S,5′R)-4′-(4-Nitrophenyl)-5′-phenyl-3′-(pyrene-1-carbonyl) spiro[indoline-3,2′-pyrrolidin]-2-one (**7e**).* Pale brown powder; mp 203–205 °C. IR (KBr): ν_{max} = 3349 (NH), 3185 (NH), 3028 (CH arom.), 2946 (CH aliph.), 1715 (C=O), 1669 (C=O) cm^{-1}. ^{1}H NMR (400 MHz, DMSO-d_6): δ 9.97 (s, 1H, N_1–H), 8.34–8.22 (m, 3H), 8.20 (d, J = 8.5 Hz, 2H, $C_{3''}$–H), 8.17–8.02 (m, 4H), 8.00–7.85 (m, 2H), 7.80 (d, J = 8.4 Hz, 2H, $C_{2''}$–H), 7.62 (d, J = 7.3 Hz, 1H, C_4–H), 7.44 (d, J = 7.3 Hz, 2H, $C_{5'b}$–H), 7.30 (d, J = 7.3 Hz, 2H, $C_{5'c}$–H), 7.27–7.26 (m, 1H, $C_{5'd}$–H), 6.96 (t, J = 7.5 Hz, 1H, C_5–H), 6.73 (t, J = 7.6 Hz, 1H, C_6–H), 5.98 (d, J = 7.7 Hz, 1H, C_7–H), 5.17 (d, J = 11.2 Hz, 1H, $C_{3'}$–H), 5.04 (d, J = 10.3 Hz, 1H, $C_{5'}$–H), 4.33 (t, J = 10.7 Hz, 1H, $C_{4'}$–H), 4.12 (br, 1H, $N_{1'}$–H) ppm. ^{13}C NMR (100 MHz, DMSO-d_6): δ (ppm) 199.6 ($C_{1'''}$), 180.8 (C_2), 147.3 ($C_{4''}$–NO_2), 146.5 ($C_{1''}$), 141.2 (C_{7a}), 141.0 ($C_{5'a}$), 133.3 (C), 131.4 (C), 130.6 (C_{3a}), 130.5 (C), 129.9 ($C_{2''}$–H), 129.8 (C), 129.7 (C–H), 128.7 (C–H), 128.5 (C), 128.4 (C_6–H), 128.3 ($C_{5'c}$–H), 127.7 (CH), 127.4 ($C_{5'd}$H), 127.2 ($C_{5'b}$–H), 127.0 (CH), 126.7 (C–H), 126.4 ($C_{3'''}$–H), 126.1 (C_4–H), 126.0 (CH), 124.0 (CH), 123.6 ($C_{3''}$–H), 123.5 (C), 123.1 (CH), 123.0 (C), 122.1 (C_5–H), 109.0 (C_7–H), 67.8 (C_3/$C_{2'}$), 67.6 ($C_{5'}$–H), 64.4 ($C_{3'}$–H), 55.6 ($C_{4'}$–H) ppm.

*(3S,3′R,4′S,5′R)-4′-(4-Cyanophenyl)-5′-phenyl-3′-(pyrene-1-carbonyl) spiro[indoline-3,2′-pyrrolidin]-2-one (**7f**).* Yellow powder; mp 199–201 °C. IR (KBr): ν_{max} = 3335 (NH), 3185 (NH), 3049 (CH arom.), 2957 (CH aliph.), 2226 (CN), 1716 (C=O), 1670 (C=O) cm^{-1}. ^{1}H NMR (400 MHz, DMSO-d_6): δ 9.92 (s, 1H, N_1–H), 8.27–7.97 (m, 7H), 7.91 (d, J = 9.3 Hz, 1H, C–H), 7.83 (d, J = 9.2 Hz, 1H, C–H), 7.75 (d, J = 8.0 Hz, 2H, $C_{3''}$–H), 7.67 (d, J = 8.0 Hz, 2H, $C_{2''}$–H), 7.56 (d, J = 7.3 Hz, 1H, C_4–H), 7.37 (d, J = 7.3 Hz, 2H, $C_{5'b}$–H), 7.26 (d, J = 7.3 Hz, 2H, $C_{5'c}$–H), 7.24–7.16 (m, 1H, $C_{5'd}$–H), 6.90 (t, J = 7.6 Hz, 1H, C_5–H), 6.68 (t, J = 7.6 Hz, 1H, C_6–H), 5.94 (d, J = 7.6 Hz, 1H, C_7–H), 5.09 (d, J = 11.1 Hz, 1H, $C_{3'}$–H), 4.97 (dd, J = 10.2, 5.4 Hz, 1H, $C_{5'}$–H), 4.23 (t, J = 10.7 Hz, 1H, $C_{4'}$–H), 4.05 (d, J = 5.4 Hz, 1H, $N_{1'}$–H) ppm. ^{13}C NMR (100 MHz, DMSO-d_6): δ 199.7 ($C_{1'''}$), 180.9 (C_2), 145.2 ($C_{1''}$), 141.2 (C_{7a}), 141.1 ($C_{5'a}$), 133.3 (C), 132.4 ($C_{3''}$–H), 131.4 (C), 130.6 (C_{3a}), 130.4 (C), 129.7 (C_2), 129.6 ($C_{2''}$–H & CH overlapping), 128.6 (C_6–H), 128.5 (C), 128.4 (C–H), 128.2 ($C_{5'c}$–H), 127.6 ($C_{5'd}$–H), 127.2 ($C_{5'b}$–H), 127.0 (C–H), 126.6 (C–H), 126.3 ($C_{3'''}$–H), 126.0 (C_4–H & 2CH overlapping), 124.0 (CH), 123.8 (C_3–H), 123.5 (C), 123.0 (C), 121.9 (C_5–H), 118.8 (CN), 109.8 ($C_{4''}$), 109.0 (C_7–H), 67.8 (C_3/$C_{2'}$), 67.5 ($C_{5'}$–H), 64.3 ($C_{3'}$–H), 55.8 ($C_{4'}$–H) ppm.

Conflicts of interest

There are no conflicts to declare.

Acknowledgements

The authors are highly indebted to the Deanship of the Scientific Research (DSR), Umm Al-Qura University for full financial support of this work through the project number 15-SCI-3-1-0010. S. A. Ahmed is highly indebted to Alexander von Humboldt Foundation (AvH) and Prof. Jochen Mattay, Bielefeld University, Germany for helping with some analytical and spectroscopic measurements in addition to some labwares donations.

Notes and references

1 (*a*) I. Ugi, A. Dömling and W. Hörl, *Endeavour*, 1994, **18**, 115–122; (*b*) S. L. Dax, J. J. McNally and M. A. Youngman, *Curr. Med. Chem.*, 1999, **6**, 255–270; (*c*) L. Weber, K. Illgen and M. Almstetter, *Synlett*, 1999, 366–374; (*d*) A. Dömling, *Curr. Opin. Chem. Biol.*, 2002, **6**, 303–313; (*e*) L. Weber, *Drug Discovery Today*, 2002, **7**, 143–147; (*f*) E. M. Hussein, *Z. Naturforsch.*, 2012, **67b**, 231–237; (*g*) A. Dömling, W. Wang and K. Wang, *Chem. Rev.*, 2012, **112**, 3083–3135; (*h*) E. M. Hussein, *Monatsh. Chem.*, 2013, **144**, 1691–1697; (*i*) E. M. Hussein, *Russ. J. Org. Chem.*, 2015, **51**, 54–64; (*j*) E. M. Hussein and S. A. Ahmed, *Chem. Heterocycl. Compd.*, 2017, **53**, 1148–1155.

2 (*a*) F. Shi, R. Mancuso and R. C. Larock, *Tetrahedron Lett.*, 2009, **50**, 4067–4070; (*b*) F. Shi, R. Zhu, X. Liang and S. Tu, *Adv. Synth. Catal.*, 2013, **355**, 2447–2458; (*c*) C. Wang, R. Zhu, J. Zheng, F. Shi and S. Tu, *J. Org. Chem.*, 2015, **80**, 512–520; (*d*) W. Dai, X. Jiang, Q. Wu, F. Shi and S. Tu, *J. Org. Chem.*, 2015, **80**, 5737–5744.

3 (*a*) A. K. Ganguly, N. Seah, V. Popov, C. H. Wang, R. Kuang, A. K. Saksena, B. N. Pramanik, T. M. Chan and A. F. McPhail, *Tetrahedron Lett.*, 2002, **43**, 8981–8983; (*b*) K. A. Ahrendt and R. M. Williams, *Org. Lett.*, 2004, **6**, 4539–4541; (*c*) V. Nair and T. D. Suja, *Tetrahedron*, 2007, **63**, 12247–12275; (*d*) M. Ghandi, A. Yari, S. J. T. Rezaei and A. Taheri, *Tetrahedron Lett.*, 2009, **50**, 4724–4726; (*e*) S. V. Karthikeyan, B. D. Bala, V. P. A. Raja, S. Perumal, P. Yogeeswari and D. Sriram, *Bioorg. Med. Chem. Lett.*, 2010, **20**, 350–353.

4 T. Onishi, P. R. Sebahar and R. M. Williams, *Org. Lett.*, 2003, **5**, 3135–3137.

5 M. N. G. James and G. J. B. Williams, *Can. J. Chem.*, 1972, **50**, 2407–2412.

6 A. Jossang, P. Jossang, H. A. Hadi, T. Sevenet and B. Bodo, *J. Org. Chem.*, 1991, **56**, 6527–6530.

7 N. Anderton, P. A. Cockrum, S. M. Colegate, J. A. Edgar, K. Flower, I. Vit and R. I. Willing, *Phytochemistry*, 1998, **48**, 437–439.

8 T. H. Kang, K. Matsumoto, Y. Murakami, H. Takayama, M. Kitajima, N. Aimi and H. Watanabe, *Eur. J. Pharmacol.*, 2002, **444**, 39–45.

9 T. Usui, M. Kondoh, C.-B. Cui, T. Mayumi and H. Osada, *Biochem. J.*, 1998, **333**, 543–548.

10 M. J. Kornet and A. P. Thio, *J. Med. Chem.*, 1976, **19**, 892–898.

11 K. Ding, Y. Lu, Z. Nikolovska-Coleska, G. Wang, S. Qiu, S. Shangary, W. Gao, D. Qin, J. Stuckey, K. Krajewski, P. P. Roller and S. Wang, *J. Med. Chem.*, 2006, **49**, 3432–3435.

12 J. W. Skiles and D. McNeil, *Tetrahedron Lett.*, 1990, **31**, 7277–7280.

13 T. D. Aicher, D. C. Knorr and H. C. Smith, *Tetrahedron Lett.*, 1998, **39**, 8579–8580.

14 J. E. Baldwin, R. T. Freeman, C. Lowe, C. J. Schofield and E. Lee, *Tetrahedron*, 1989, **45**, 4537–4550.

15 G. Trapani, M. Franco, A. Latrofa, A. Carotti, S. Cellamare, M. Serra, C. A. Ghiani, G. Tuligi, G. Biggio and G. Liso, *J. Pharm. Pharmacol.*, 1996, **48**, 834–840.

16 (*a*) S. R. Murugan, S. Anbazhagan and S. Narayanan, *Eur. J. Med. Chem.*, 2009, **44**, 3272–3279; (*b*) K. Karthikeyan, R. S. Kumar, D. Muralidharan and P. T. Perumal, *Tetrahedron Lett.*, 2009, **50**, 7175–7179; (*c*) A. S. Girgis, *Eur. J. Med. Chem.*, 2009, **44**, 91–100; (*d*) R. R. Kumar, S. P. S. C. Manju, P. Bhatt, P. Yogeeswari and D. Sriram, *Bioorg. Med. Chem. Lett.*, 2009, **19**, 3461–3465.

17 (*a*) L. R. Domingo, M. J. Aurell, P. Perez and R. Contreras, *Tetrahedron*, 2002, **58**, 4417–4423; (*b*) L. R. Domingo, M. J. Aurell, P. Perez and R. Contreras, *Tetrahedron*, 2003, **59**, 3117–3125; (*c*) P. Arroyo, M. T. Picher and L. R. Domingo, *J. Mol. Struct.*, 2004, **709**, 45–52; (*d*) P. Arroyo, M. T. Picher, L. R. Domingo and F. Terrier, *Tetrahedron*, 2005, **61**, 7359–7365.

18 (*a*) L. R. Domingo, *Molecules*, 2016, **21**, 1; (*b*) M. Hamzehloueian and Z. Davari, *J. Mol. Graphics Modell.*, 2018, **80**, 32–37.

19 J. Weng, Q. Mei, Q. Q. Ling, Q. Fan and W. Huang, *Tetrahedron*, 2012, **68**, 3129–3134.

20 E. M. Hussein, S. A. Ahmed and I. I. Althagafi, *Heterocycl. Commun.*, 2017, **23**, 379–384.

21 (*a*) E. M. Hussein and M. I. Abdel-Monem, *ARKIVOC*, 2011, **10**, 85–98; (*b*) E. M. Hussein, S. A. Ahmed, N. El Guesmi and K. S. Khairou, *J. Chem. Res.*, 2017, **41**, 346–351.

22 (*a*) R. R. Kumar, S. Perumala, P. Senthilkumar, P. Yogeeswari and D. Sriram, *Eur. J. Med. Chem.*, 2009, **44**, 3821–3829; (*b*) J. He, G. Ouyang, Z. Yuan, R. Tong, J. Shi and L. Ouyang, *Molecules*, 2013, **18**, 5142–5154.

23 Y. Sarrafi, M. Hamzehloueian, K. Alimohammadi and S. Yeganegi, *J. Mol. Struct.*, 2012, **1030**, 168–176.

24 (*a*) F. De Proft and P. Geerlings, *Chem. Rev.*, 2001, **101**, 1451–1464; (*b*) P. Geerlings, F. De Proft and W. Langenaeker, *Chem. Rev.*, 2003, **103**, 1793–1873; (*c*) P. W. Ayers, J. S. M. Anderson and L. J. Bartolotti, *Int. J. Quantum Chem.*, 2005, **101**, 520–534; (*d*) J. L. Gázquez, *J. Mex. Chem. Soc.*, 2008, **52**, 3–10; (*e*) P. Geerlings, S. Fias, Z. Boisdenghien and F. De Proft, *Chem. Soc. Rev.*, 2014, **43**, 4989–5008.

25 M. Rahm and T. Brinck, *J. Phys. Chem. A*, 2008, **112**, 2456–2461.

26 (*a*) R. G. Parr and W. Yang, *Density Functional Theory of Atoms and Molecules*, Oxford University Press, New York, 1989; (*b*)

R. G. Parr, L. von Szentpaly and S. Liu, *J. Am. Chem. Soc.*, 1999, **121**, 1922–1924.

27 (*a*) P. Pérez, L. R. Domingo and A. Aizman, in The electrophilicity index in organic chemistry, *Theoretical aspects of chemical reactivity*, ed. A. Toro-Labbe, Elsevier, Amsterdam, 2007, vol. 9, pp.139–201; (*b*) P. Pérez, L. R. Domingo, M. J. Aurell and R. Contreras, *Tetrahedron*, 2003, **59**, 3117–3125; (*c*) P. Pérez, L. R. Domingo, M. Duque-Noreña and E. Chamorro, *J. Mol. Struct.*, 2009, **895**, 86–91.

28 (*a*) L. R. Domingo, M. J. Aurell, P. Perez and R. Contreras, *Tetrahedron*, 2002, **58**, 4417–4423; (*b*) P. Arroyo, M. T. Picher and L. R. Domingo, *J. Mol. Struct.*, 2004, **709**, 45–52; (*c*) P. Arroyo, M. T. Picher, L. R. Domingo and F. Terrier, *Tetrahedron*, 2005, **61**, 7359–7365; (*d*) D. V. Steglenko, M. E. Kletsky, S. V. Kurbatov, A. V. Tatarov, V. I. Minkin, R. Goumont and F. Terrier, *J. Phys. Org. Chem.*, 2008, **22**, 298–307; (*e*) S. Lakhdar, F. Terrier, D. Vichard, G. Berionni, N. El Guesmi, R. Goumont and T. Boubaker, *Chem.–Eur. J.*, 2010, **16**, 5681–5690.

29 C. Hansch, A. Leo and R. W. Taft, *Chem. Rev.*, 1991, **91**, 165–195.

30 H. Ayouchia, H. Anane, M. L. I. Moubtassim, L. R. Domingo, M. Julve and S. Stiriba, *Molecules*, 2016, **21**, 1434.